AECL

Canadian Nuclear Society

CANDU FUEL FOR THE FUTURE

COMBUSTIBLE CANDU POUR L'AVENIR

IAEA

Zircatec Precision Industries Inc.

GE Canada Nuclear Products

ONTARIOPOWER GENERATION

Hydro Québec

CONFERENCE PROCEEDINGS Vol.1

Vol.1: ISBN 0-919784-70-4
Vol.2: ISBN 0-919784-71-2

Seventh International Conference on CANDU Fuel
2001 September 23-27
Kingston, Ontario

7ième Conférence internationale sur le combustible CANDU
23-27 sept. 2001
Kingston, Ontario

CANADIAN NUCLEAR SOCIETY: SEVENTH INTERNATIONAL CONFERENCE ON CANDU FUEL

2001 September 23-27, Kingston, Ontario, Canada

Sponsored/Supported by: Atomic Energy of Canada Limited, General Electric Canada, Hydro Québec, International Atomic Energy Agency, Ontario Power Generation, Royal Military College of Canada and Zircatec Precision Industries

CONFERENCE PROCEEDINGS
VOLUME 1

B.J. Lewis, Editor

ORGANIZING COMMITTEE

Conference Chair:	Brent Lewis
Program Co-Chairs:	Fernando Iglesias, Erl Kohn & Mukesh Tayal
Conference Secretary:	Hugues Bonin
Program Secretary:	Paul Chan & Leslie Bennett
Sponsorship & Publicity Coordinator:	Bill Andrews
Facilities Coordinator:	Trish Lewis
Treasurer & Registration:	Denise Rouben
Photographer:	Bernie Surette

Published by the Canadian Nuclear Society, 2001, Toronto
Copyright © Canadian Nuclear Society, 480 University Ave., Suite 200, Toronto, Ontario, Canada M5G 1V2
Contact: D. Rouben, Tel: (416) 977-7620, Fax: (416) 977-8131, email: cns-snc@on.aibn.com

Vol 1: ISBN 0-919784-70-4
Vol 2: ISBN 0-919784-71-2

MICROCHEMICAL STUDIES OF IRRADIATED FUEL BY IMAGING-XPS

W.H. HOCKING and K.G. IRVING

Corrosion and Surface Science Branch
Atomic Energy of Canada Limited (AECL)
Chalk River Laboratories, Chalk River, Ontario, CANADA, K0J 1P0

ABSTRACT

An advanced facility for characterization of highly radioactive materials by Imaging X-ray Photoelectron Spectroscopy (XPS) has recently been commissioned at the Chalk River Laboratories. Microchemical analysis of areas as small as 20 μm in diameter and chemical-state imaging with a spatial resolution of ~3 μm can be achieved. An auxiliary Schottky field-emission electron gun also offers high-performance *in situ* capabilities for scanning electron microscopy (SEM) and scanning Auger microscopy (SAM). Based upon experience gained over the previous decade using a prototype active XPS system, the new facility has been configured to allow safe examination of irradiated-fuel samples. The pumping system and sample-preparation chambers were custom-designed to prevent internal migration or release of radioactive contamination and to allow diverse experiments under ultra-high-vacuum conditions. Preliminary results from an initial study of the fuel-sheath interface in a fuel element that was irradiated in a CANDU[1] power reactor are presented to illustrate the potential applications of the active Imaging-XPS facility. New insight into fission-product segregation and CANLUB degradation processes has already begun to emerge that should permit development of improved barrier systems on advanced CANDU fuels.

1. INTRODUCTION

Reliable fuel performance to extended burnup will be required to fully exploit the advanced fuel cycles that are feasible in CANDU reactors because of their high neutron economy [1]. Significant improvements in fuel science could be achieved through better control of the chemistry at interfaces within the fuel element [2-5]. Fission products that have limited solubility in the fuel matrix tend to segregate to grain boundaries, from whence they can readily migrate to the sheath [2-7]. These processes are strongly dependent upon burnup and element power as well as the fuel-bundle design. Several fission products have been implicated in fuel failures caused by stress-corrosion cracking (SCC) of the Zircaloy-4 sheath [8]. Transport of fission products from defected fuel elements throughout the heat-transport system of operating reactors can contribute significantly to occupational radiation exposures. Accumulation of segregated fission products on the fuel grain boundaries and at the fuel-sheath interface also enhances the potential for release of radioactivity to the environment during postulated reactor accidents and from used fuel in storage or after disposal [2-5].

[1] CANDU (CANada Deuterium Uranium) is a registered trademark of AECL.

The thin CANLUB graphite coating applied to the sheath interior surface has proven to be extremely successful in preventing SCC for the modest burnups that are currently achieved with natural-uranium fuels in CANDU power reactors [8]. Although graphite is effective as a pellet lubricant in reducing sheath stress, the CANLUB layer has been shown to play a more important role as a fission-product chemical barrier [8]. There is also considerable evidence that it controls reaction of fission-freed oxygen with the sheath, which in turn may have a profound impact on the chemical speciation and migration of several key fission products [7,9-12]. Progressive degradation of the integrity of the CANLUB layer with increasing burnup has been well documented [9]. Some progress has recently been achieved in understanding the mechanisms involved in the function and degradation of the CANLUB layer, which could lead to the development of a more robust barrier system [10,11].

Exploratory studies of the chemistry at the grain boundaries and the fuel-sheath interface in irradiated CANDU fuels have been conducted over the past decade using a prototype active X-ray photoelectron spectrometer (XPS) located at the Whiteshell Laboratories [11,13-15]. Segregation of a number of fission products to the fuel grain boundaries was explicitly demonstrated for the first time [14]. Exposure of used CANDU fuel to warm, moist air—simulating canister storage of defected elements—was also shown to cause pervasive but highly selective grain-boundary oxidation [15]. Despite the severe limitations of a comparatively large analysis area and lack of any *in situ* imaging capability, general aspects of the complex layer that develops at the fuel-sheath interface were revealed [11]. In particular, carbon was confirmed to remain the predominant constituent here even at high burnup, although segregated fission products and recoil-implanted fuel become increasingly important as well. These studies are now being pursued using an advanced Imaging-XPS instrument that was recently commissioned at the Chalk River Laboratories (CRL) for characterization of highly radioactive materials.

2. ACTIVE IMAGING-XPS FACILITY

The modern active Imaging-XPS facility at CRL is based upon an ESCALAB 220i-XL instrument manufactured by VG Scientific. Microchemical surface analysis of areas as small as 20 μm in diameter can be performed in the spectroscopy mode, which employs six channel-electron multipliers to achieve high sensitivity and wide dynamic range. Alternatively, photoelectron images of an element in a particular chemical state can be collected on a position-sensitive detector (two microchannel plates in a chevron configuration followed by a phosphor screen and a CCD camera) [16-18]. A spatial resolution of ~3 μm can be achieved in this mode, which provides optimum throughput for imaging by simultaneous detection of the entire field of view—analogous to an optical microscope [16-18]. In either case, a computer-controlled electron spectrometer, which consists of magnetic and electrostatic lenses and a concentric hemispherical analyzer, yields exceptional photoelectron collection efficiency and high energy resolution. A choice of three X-ray sources offers flexibility in the selection of photoelectron emission area and energy (which determines the sampling depth) and permits shifting of Auger electron peaks to identify or avoid spectral interferences. Areas larger than ~1 cm^2 can be irradiated with characteristic Mg $K\alpha$ or Zr $L\alpha$ and Zr $M\zeta$ X-rays ($h\nu$ = 1253.6 eV, 2042.4 eV and 151.4 eV respectively) from a simple twin-anode source, although some Bremsstrahlung

radiation and satellite X-rays are also generated [19]. A focussed beam of X-rays (adjustable in diameter from ~100 μm to ~1 mm) with high spectral purity is produced by a monochromator that uses a pair of bent silicon crystals to filter Al Kα radiation ($h\nu$ = 1486.6 eV). The photoelectron escape depth can also be varied (over the <5 nm range) by changing the take-off angle using the microprocessor-controlled 5-axis precision sample stage [19]. A magnified real-time image of the sample in the analysis position, which is produced by a CCD camera mounted on an optical microscope, is displayed on two video monitors. An auxiliary Schottky field-emission electron gun provides *in situ* capabilities for scanning electron microscopy (SEM) and scanning Auger microscopy (SAM), with a spatial resolution of better than 100 nm.

Studies of radioactive materials are facilitated by various aspects of the instrument design, including special modifications as well as intrinsic features. The sensitive XPS imaging and spectroscopy detectors are located at a distance of ~1 m from the sample-analysis position and shielded by massive electron-optics components constructed out of Mumetal and stainless steel. A protective shield has been fitted on the secondary-electron detector that is used for SEM imaging to prevent excitation or damage by α and β particles. Samples normally enter the instrument from the laboratory through an introduction chamber that is connected via a preparation chamber to the analysis chamber. The preparation chamber is equipped with two custom-designed pocket chambers, in which diverse experiments on radioactive materials can be conducted, including fracture, ion-sputter etching and exposure to reactive gases while heating or cooling. A portable stainless steel vessel, which will mate with the introduction-chamber port, can also be used to transport samples from a remote location (e.g., an anaerobic chamber) under high vacuum or an inert atmosphere. Each chamber is separately pumped and can be isolated with gate valves: the double-isolation strategy followed here ensures that radioactive contamination is largely confined to the pocket chambers, which can be cleaned most easily. A manipulator mounted on the preparation chamber allows samples, attached to sample-transfer mounts, to be securely moved from one chamber to another. Ultra-high vacuum is normally maintained in the analysis, preparation and pocket chambers using a combination of sputter-ion, titanium-sublimation and maglev-turbomolecular pumps. The introduction chamber, which is frequently vented to atmospheric pressure, is evacuated to high vacuum by a conventional turbomolecular pump. The rotary-vane pumps that back the turbomolecular pumps are exhausted through a HEPA filter into the building active-duct system. All gas flow is filtered and controlled when any part of the instrument is vented to, or pumped from, atmospheric pressure to prevent internal migration or release of radioactive contamination.

The Imaging-XPS instrument has been installed in a Class B radioisotope laboratory that is located in the same building as a number of other key active facilities, including hot cells. A shielded radiological fumehood, which is situated in an alcove connected to the main laboratory, is used for maintenance work on contaminated instrument components and mounting radioactive samples. Any α and β particles emitted by a radioactive sample within the XPS vacuum system will be entirely absorbed in the chamber walls, whereas γ-rays are attenuated by less than a factor of two. However, the γ-ray field produced by a small sample decreases approximately as a function of the distance squared, and provision of extended cables has allowed the vacuum system to be separated by ~3 m from the instrument computer and electronics. Further attenuation of the γ-ray field from a high-intensity source, by about an order of magnitude, can be achieved by strategically positioning four moveable shields, which are suspended from an

overhead track. The radiation design limit for the Imaging-XPS laboratory is a sample with a γ-ray field of 10 R/h (0.1 Gy/h) measured at a distance of ~100 mm. Additional radiological fumehoods, shielded storage blocks and an active secondary ion mass spectrometer (SIMS) are located in adjacent Class B laboratories, creating an integrated facility for radioactive materials characterization.

The vacuum system of the Imaging-XPS instrument is shown in Figure 1; key components that are labelled by numbered arrows on this photograph are discussed further below. The electronics racks and the operator's console are entirely outside the field of view here. One of the moveable γ-radiation shields has been parked behind the analysis chamber (in left centre of the photograph) and part of its support structure is visible (1), suspended from the overhead track, above and beyond the large hemispherical vacuum chamber that contains the electron analyzer (2). The Schottky field-emission electron gun, which is equipped with an auxiliary ion pump (3), projects from the analysis chamber into the left foreground, just in front of the video camera (4). Several of the stepping motors on the five-axis, remotely controlled, sample stage are visible at the far end of the vacuum system, whereas the X-ray sources are largely hidden behind the analysis chamber and the electron optics column, which extends up to the electron analyzer. The sample-introduction chamber is clearly visible near the centre of the photograph (5) and one of the pocket chambers, upon which a fracture stage (6) has been mounted, projects into the right foreground. Portions of the carousel preparation chamber and the second pocket chamber, which is equipped with an ion gun (7), a heating/cooling stage and a gas-introduction system, can be identified behind the fracture-stage chamber.

3. INITIAL APPLICATION TO CANDU FUEL

An initial study of the microchemistry at the fuel-sheath interface in a conventional CANDU fuel was undertaken using the active Imaging-XPS instrument on element 2 from bundle B64996C, which had been irradiated in the Point Lepreau nuclear generating station to an outer-element burnup of 230 MW·h/kg U at linear-power ratings of 40-48 kW/m [20]. Although this bundle included several non-CANLUB outer elements, the inner sheath surface on element 2 had been coated with a standard, graphite-based CANLUB layer [20]. The peak outer-element power of ~48 kW/m was achieved early in the irradiation (increased from ~44 kW/m by a bundle shift) and thereafter the power declined slowly to ~40 kW/m at discharge. Previously developed procedures, which involve only dry-cutting techniques, were employed to obtain sheath samples with minimum risk of surface alteration or contamination [11,13-15]. Complete element segments, ~2 cm long, were cut first using a high-speed silicon carbide saw. The sheath was then gently removed from the fuel in two half-cylinders after two further high-speed axial cuts. Finally, appropriately sized samples (~5 mm by ~7 mm) were cut from near the centre of the half-cylinders using a slow-speed diamond saw operated with minimum pressure. A similar strategy was followed to obtain a sample from the end cap at the reference end of the element. As illustrated in Figure 2, the specimens were securely captured within a recessed area on a custom-designed sample-transfer mount before being introduced into the Imaging-XPS instrument. This photograph was taken through a view port (hidden behind the electron gun in Figure 1) located on the left-front side of the analysis chamber. Several electron optics components (e.g., electron gun and photoelectron extraction lens) project into the field of view

from above, and the top of an electromagnetic immersion lens is visible below the precision sample stage. The curved surface of the fuel-sheath specimen (at the tip of the arrow) is clearly visible through a rectangular hole in the metal cover plate that captures it within the shallow well on the sample-transfer mount (attached to the end of the stage near the centre of the photograph).

The *in situ* SEM capability of the Imaging-XPS instrument was routinely used to identify and select various features on the sheath and end-cap samples for microchemical analysis. Illustrative examples of the morphologies seen on the inside surface of the B64996C/2 sheath at a typical location and at a former pellet-pellet interface have been displayed in Figures 3 and 4 respectively. An area ~500 μm in diameter, centred on a selected feature, was irradiated with monochromatic Al Kα X-rays and the photoelectron lens system was used to restrict the XPS analysis region to <150 μm diameter. The dispersion and work function of the photoelectron spectrometer were calibrated using gold, silver and copper standards, with the binding-energy scale referenced to the Fermi level [21]. Information on the near-surface composition as a function of depth was compiled by sequential XPS analysis and argon-ion sputtering; the latter was done remotely (at location 7 on Figure 1) to prevent radioactive contamination of sensitive detectors in the analysis chamber. A focussed 4 keV ion beam, with an Ar^+ current of 1.3 μA, was incident on the sample approximately normal to the surface and was rastered over an area of 5 mm by 7 mm. Under these conditions, the sputter rate has been determined to be 0.5 nm/min using an oxide thin-film standard [22].

The light-grey and dark-grey areas observed in Figure 3 (as well as in Figure 4) appear to have thin and thick retained CANLUB layers respectively (discussed further below). Representative XPS survey spectra that were recorded from typical locations on the inside sheath surface, with evident thin and thick retained CANLUB layers, have been reproduced in Figure 5. In both cases, the C 1s emission has produced the strongest peak in the spectrum—consistent with graphite being the predominant constituent at the surface—despite the fact that it has a small X-ray photoelectron cross-section [19]. Segregated fission products, notably Cs, Ba and Xe, have been detected only at quite low levels. The intensities of the zirconium peaks are surprisingly similar in the two spectra, whereas the most significant difference between them is the relatively strong U 4f emission from the area with the thin retained CANLUB layer. Weaker zirconium photoelectron emission might have been expected from the area with the thick retained CANLUB layer.

An XPS survey spectrum that was recorded from the thick patch of CANLUB seen in Figure 4, adjacent to a former pellet-pellet interface, has been displayed in Figure 6. Exceptionally high levels of segregated fission products, including Cs, Ba, I, Cd and Rb, have been found here (and confirmed by additional XPS analyses at other locations on the same feature). The relative intensities of the peaks arising from C, U and Zr in Figure 6 are comparable with those in the lower spectrum of Figure 5, despite the marked differences between the two regions in other respects. Elevated concentrations of segregated fission products were commonly detected at additional locations on, or near, former pellet-pellet interfaces, including the nearly white band in Figure 4, but more typically at levels intermediate between the extremes of Figures 5 and 6.

Illustrative portions of XPS spectra that were recorded, after increasing intervals of argon-ion sputtering, from an area with a thin retained CANLUB layer (same location as the lower

spectrum in Figure 5) have been displayed in Figure 7. The relative intensity of the U 4f spin-orbit doublet increases rapidly after the initial few minutes of sputtering (as adventitious contamination from air exposure is removed) and then slowly decreases thereafter (followed, but not shown, out to 100 min). Conversely, the strength of the Zr emission features progressively increases as a function of sputter time (with the Zr 3d doublet exceeding the C 1s peak after 100 min). Chemical-shift effects in Figure 7 indicate almost complete reduction of zirconium and partial reduction of uranium, to the elemental state, after 60 min of argon-ion sputtering [23]. Even greater reduction of uranium was found following 100 min of sputtering (data not shown); these observations will be discussed further in the next section. Comparable depth profiles at locations with thick retained CANLUB layers revealed only subtle changes—most notably, a progressive, albeit modest, increase in the strength of the U 4f doublet.

Segments of XPS spectra (high binding energy range) that were recorded, after increasing intervals of argon-ion sputtering, from the thick CANLUB patch identified in Figure 4 (adjacent to the pellet-pellet interface) have been reproduced in Figure 8. The intensities of the emission peaks arising from segregated fission products decrease by about a factor of two after 9 min of sputtering and then much more slowly thereafter (following an initial increase again due to removal of adventitious contamination). Chemical-shift effects for the Cs 3d and I 3d doublets as well as their relative intensities throughout the depth profile suggest the presence of CsI microcrystallites plus a modest excess of cesium. The progressive increase in the strength of the U 4d doublet as a function of sputter time (a plateau level was reached after 140 min) is again consistent with migration of uranium deep into the CANLUB layer.

Secondary-electron images of the inside surface of the end-cap sample revealed extensive coverage by very fine grained deposits, which were not sufficiently thick to entirely mask the original machining marks. Key portions of XPS spectra that were recorded, after increasing intervals of argon-ion sputtering, from a typical location near the centre of the end cap have been displayed in Figure 9. A comparatively thin layer—composed predominantly of fission products, including Cs, Cd, Pd, Ag, Ba, Te, Rb and Ru—has been depth-profiled here. Chemical-shift effects indicate that the noble metals were not oxidized; they were most likely present in the form of alloy nanoparticles [12]. The depth distribution of uranium suggests migration into at least the surface oxide film on the underlying Zircaloy. Similar results, with some variability in the relative proportions of the fission products and their depth profiles, were obtained at all other end-cap locations analyzed.

4. DISCUSSION AND CONCLUSIONS

The development of an advanced Imaging-XPS facility specifically configured for analysis of highly radioactive materials has been summarized. Preliminary results from an initial study of a conventional CANDU power-reactor fuel have been used to illustrate the scope of the potential applications as well as the possibilities for improvements in fuel science and technology. Comparatively high levels of segregated fission products were found on interior surfaces of the fuel sheath near former pellet-pellet interfaces and on an end cap; however, elsewhere on the sheath only quite low levels of fission products were detected. Incorporation of uranium to some depth in the surface at all types of locations, albeit with considerable variation in concentration,

was revealed by XPS depth profiles. Marked differences in the apparent thickness of the CANLUB layer retained on sheath surfaces were observed, which likely reflect either non-uniformity in the initial coating or varying retention on the fuel pellets, although some relocation during the irradiation is also considered probable [11].

Almost complete reduction of zirconium and partial reduction of uranium, to the elemental state, was found after extended argon-ion sputtering at sheath locations with a thin retained CANLUB layer. Because UO_2 and ZrO_2 are both known to be essentially stable under argon-ion bombardment (with only slight loss of oxygen from the latter) [24], these observations suggest radiation-induced migration of uranium through the CANLUB layer and into the surface of the underlying sheath during reactor operation. The daughter nuclides created by fission have sufficient energy to traverse distances of 6-9 μm in the fuel matrix and the associated collision cascades that reach the surface of a pellet will cause recoil implantation [25,26]. Transient vaporization of urania, due to thermal-spike effects, will also occur at any location where a fission track emerges from the pellet surface [25-27].

Lattice diffusion to the fuel grain boundaries is the first stage and normally the rate-limiting step in fission-product segregation and eventual migration to the fuel-sheath interface. At the high temperatures that are achieved near the fuel centre-line, thermal diffusion rates can be quite significant. Further diffusion along the grain boundaries is generally presumed to be comparatively easy, and development of tunnels through linkage of gas bubbles on grain-boundary intersections can permit fast release of volatile species [3-5,14]. Because of the steep radial temperature gradient in operating nuclear fuels, all of these processes are vastly more efficient near the pellet centre-line than toward its periphery. Accordingly, the expected primary migration route for fission products would be axially to the pellet end and then radially to the sheath—in the absence of large cracks that can provide a short-circuit pathway. Although there will be an axial temperature gradient in the pellets located at either end of an element as well, it will be much less than the radial gradient, owing to relatively poor heat flow through the end caps. The preliminary results presented here on the local distribution of segregated fission products at the sheath on a standard CANDU fuel element are entirely consistent with this scenario. An improved CANLUB barrier system that would more effectively block access of segregated fission products to the fuel sheath should clearly be feasible.

4. ACKNOWLEDGEMENTS

The authors would like to thank the Hot Cells staff at CRL, in particular R.E. Moeller and D.V. O'Brien, for skilful work in cutting the fuel-sheath and end-cap specimens. They are also grateful to D.S. Cox, I.J. Muir and V.F. Urbanic for constructive review of the manuscript.

5. REFERENCES

1. BOCZAR P.G., "CANDU Fuel-Cycle Vision", Atomic Energy of Canada Limited Report, AECL-11937 (1998).

2. MATZKE Hj., "Atomic Transport Properties in UO_2 and Mixed Oxide $(U,Pu)O_2$", J. Chem. Soc. Faraday Trans. 2, 83, 1121-1142 (1987).
3. MATTHEWS J.R., "Technological Problems and the Future of Research on the Basic Properties of Actinide Oxides", J. Chem. Soc. Faraday Trans. 2, 83, 1273-1285 (1987).
4. JOHNSON L.H. and D.W. SHOESMITH, "Spent Fuel", in "Radioactive Waste Forms for the Future", Edited by W. LUTZE and R.C. EWING, Elsevier Science, Amsterdam, Chapter 11, 635-698 (1988).
5. GITTUS J.H., J.R. MATTHEWS and P.E. POTTER, "Safety Aspects of Fuel Behaviour During Faults and Accidents in Pressurised Water Reactors and in Liquid Sodium Cooled Fast Breeder Reactors", J. Nucl. Mater. 166, 132-159 (1989).
6. CUBICCIOTTI D. and J.E. SANECKI, "Characterization of Deposits on Inside Surfaces of LWR Cladding", J. Nucl. Mater. 78, 96-111 (1978).
7. KLEYKAMP H., "The Chemical State of the Fission Products in Oxide Fuels", J. Nucl. Mater. 131, 221-246 (1985).
8. COX B., "Pellet-Clad Interaction (PCI) Failures of Zirconium Alloy Fuel Cladding—A Review", J. Nucl. Mater. 172, 249-292 (1990).
9. FLOYD M.R., J. NOVAK and P.T. TRUANT, "Fission-Gas Release in Fuel Performing to Extended Burnups in Ontario Hydro Nuclear Generating Stations", Atomic Energy of Canada Limited Report, AECL-10636 (1992).
10. CHAN P.K., K.G. IRVING, W.H. HOCKING, A.M. DUCLOS and A.F. GERWING, "Studies of Irradiated Zircaloy Fuel Sheathing Using XPS", Atomic Energy of Canada Limited Report, AECL-11301 (1995).
11. HOCKING W.H., R. BEHNKE, A.M. DUCLOS, A.F. GERWING and P.K. CHAN, "Investigation of the CANLUB/Sheath Interface in CANDU Fuel at Extended Burnup by XPS and SEM/WDX", Proceedings of the Fifth International Conference on CANDU Fuel, Toronto, Edited by J.H. LAU, CNS, 376-392 (1997).
12. HOCKING W.H. and F.J. SZOSTAK, "Measurement of the Composition of Noble-Metal Particles in High-Burnup CANDU Fuel by Wavelength Dispersive X-Ray Microanalysis", Proceedings of the Sixth International Conference on CANDU Fuel, Niagara Falls, Edited by R. SEJNOHA, CNS, 127-142 (1999).
13. GERWING A.F., F.E. DOERN and W.H. HOCKING, "X-Ray Photoelectron Spectroscopy on Radioactive Materials Using a McPherson ESCA-36 Equipped with an SSL Position-Sensitive Detector", Surf. Interface Anal. 14, 559-566 (1989).
14. HOCKING W.H., A.M. DUCLOS and L.H. JOHNSON, "Study of Fission-Product Segregation in Used CANDU Fuel by X-Ray Photoelectron Spectroscopy (XPS) II, J. Nucl. Mater. 209, 1-26 (1994).
15. WASYWICH K.M., W.H. HOCKING, D.W. SHOESMITH and P. TAYLOR, "Differences in Oxidation Behavior of Used CANDU Fuel During Prolonged Storage in Moisture-Saturated Air and Dry Air at 150°C", Nucl. Technol. 104, 309-329 (1993).
16. COXON P., J. KRIZEK, M. HUMPHERSON and I.R.M. WARDELL, "Escascope—A New Imaging Photoelectron Spectrometer, J. Electron Spectrosc. Relat. Phenom. 52, 821-836 (1990).
17. FORSYTH N.M. and P. COXON, "The Use of Parallel Imaging ESCA to Analyse Features Smaller than 5 Microns", Fresenius J. Anal. Chem. 346, 218-222 (1993).

18. FORSYTH N.M. and P. COXON, "Use of Parallel Imaging XPS to Perform Rapid Analysis of Polymer Surfaces with Spatial Resolution <5 μm", Surf. Interface Anal. 21, 430-434 (1994).
19. BRIGGS D. and M.P. SEAH, Editors, "Practical Surface Analysis by Auger and X-Ray Photoelectron Spectroscopy", Wiley, Chichester (1983).
20. MONTIN J., M.R. FLOYD, Z. HE and E. KOHN, "Performance of Two CANDU-6 Fuel Bundles Containing CANLUB and Non-CANLUB Production Elements", Proceedings of the Seventh International Conference on CANDU Fuel, Kingston, Edited by H.W. BONIN, CNS, (2001).
21. SEAH M.P., I.S. GILMORE and G. BEAMSON, "XPS: Binding Energy Calibration of Electron Spectrometers 5—Re-evaluation of the Reference Energies", Surf. Interface Anal. 26, 642-649 (1998).
22. HOCKING W.H., R.A. VERRALL, P.G. LUCUTA and Hj. MATZKE, "Depth-Profiling Studies of Ion-Implanted Cesium and Rubidium in SIMFUEL and Uranium Dioxide", Radiat. Effects Defects in Solids, 125, 299-321 (1993).
23. MOULDER J.F., W.F. STICKLE, P.E. SOBOL and K.D. BOMBEN, "Handbook of X-Ray Photoelectron Spectroscopy", Edited by J. CHASTAIN and R.C. KING, Jr., Physical Electronics, Eden Prairie (1995).
24. KELLY R. "On the Problem of Whether Mass or Chemical Bonding is More Important to Bombardment-Induced Compositional Changes in Alloys and Oxides", Surf. Sci. 100, 85-107 (1980).
25. MATZKE Hj., "Radiation Damage in Crystalline Insulators, Oxides and Ceramic Nuclear Fuels", Radiat. Effects, 64, 3-33, (1982).
26. MATZKE Hj., "Radiation Enhanced Diffusion in UO_2 and $(U,Pu)O_2$", Radiat. Effects, 75, 317-325, (1983).
27. WISS T., Hj. MATZKE, C. TRAUTMANN, M. TOULEMONDE and S. KLAUMUNZER, "Radiation Damage in UO_2 by Swift Heavy Ions", Nucl. Instrum. Methods Phys. Res. B, 122, 583-588 (1997).

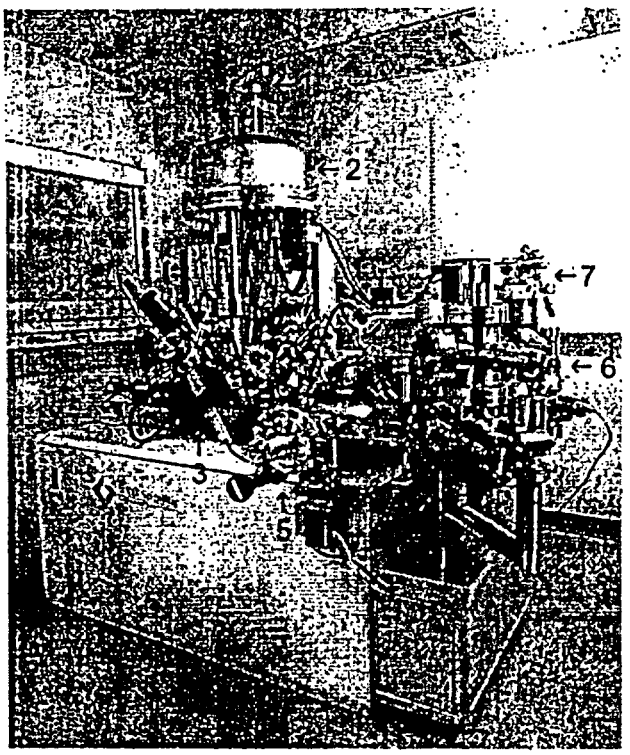

FIGURE 1. VACUUM SYSTEM OF ACTIVE IMAGING-XPS INSTRUMENT.

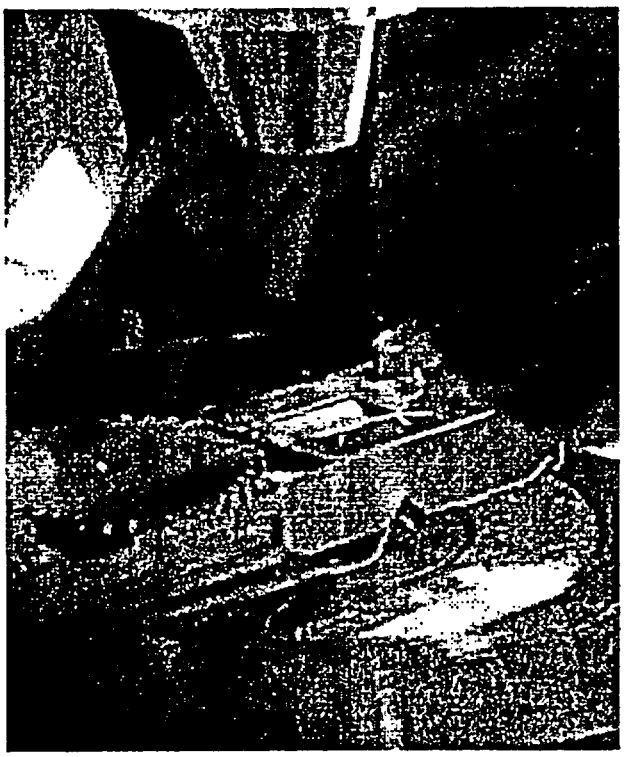

FIGURE 2. FUEL-SHEATH SAMPLE IN IMAGING-XPS ANALYSIS CHAMBER.

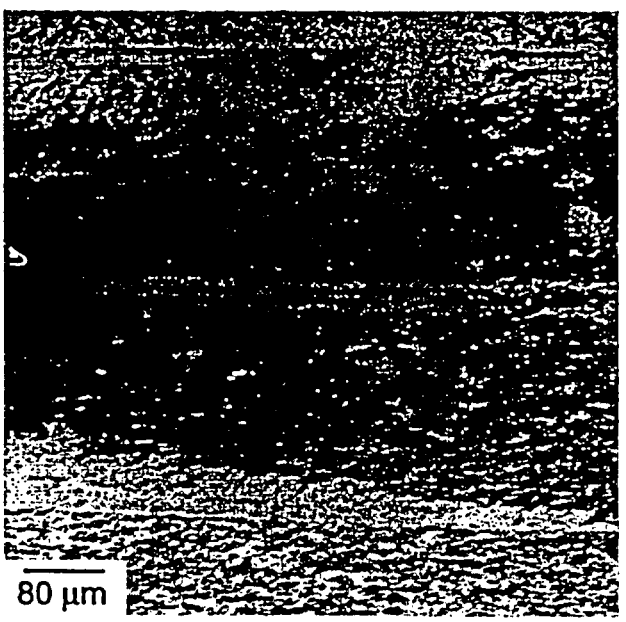

FIGURE 3. SEM IMAGE OF TYPICAL SHEATH INSIDE SURFACE.

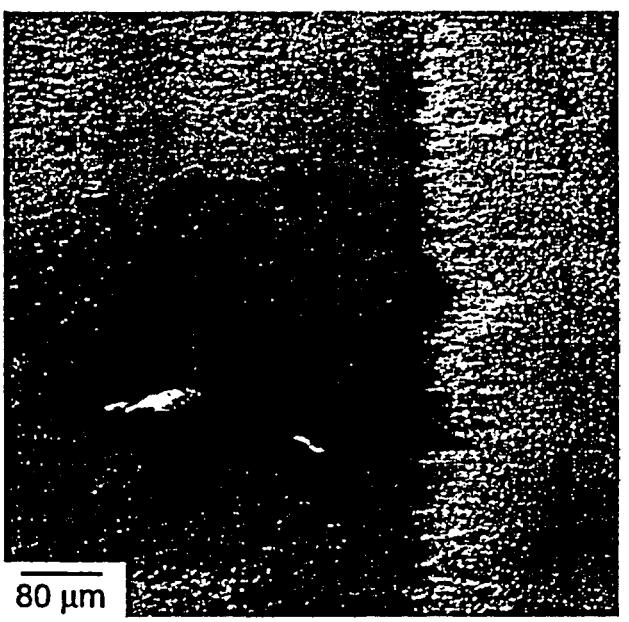

FIGURE 4. SEM IMAGE OF SHEATH AT FORMER PELLET-PELLET INTERFACE.

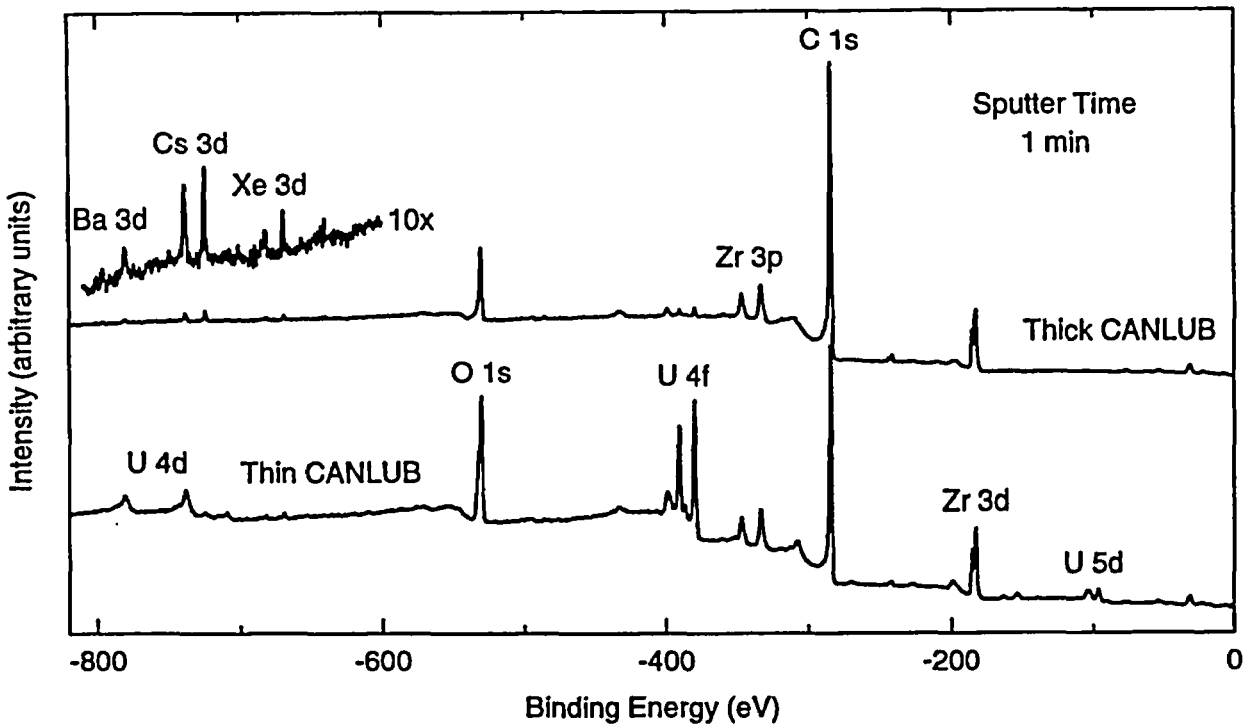

FIGURE 5. XPS SURVEY SPECTRA RECORDED FROM TYPICAL REGIONS ON FUEL SHEATH WITH THICK AND THIN CANLUB LAYERS AS SEEN IN FIGURE 3.

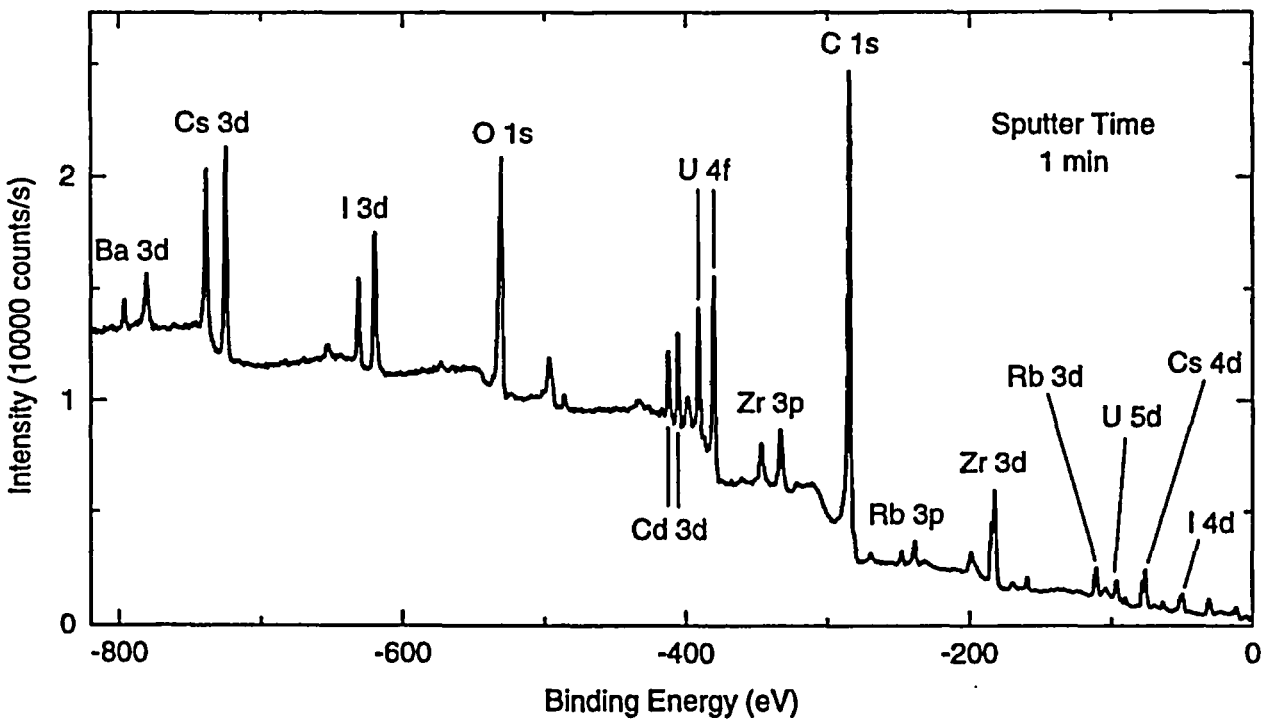

FIGURE 6. XPS SURVEY SPECTRUM RECORDED NEAR THE CENTRE OF FIGURE 4 (FROM THE THICK PATCH OF CANLUB).

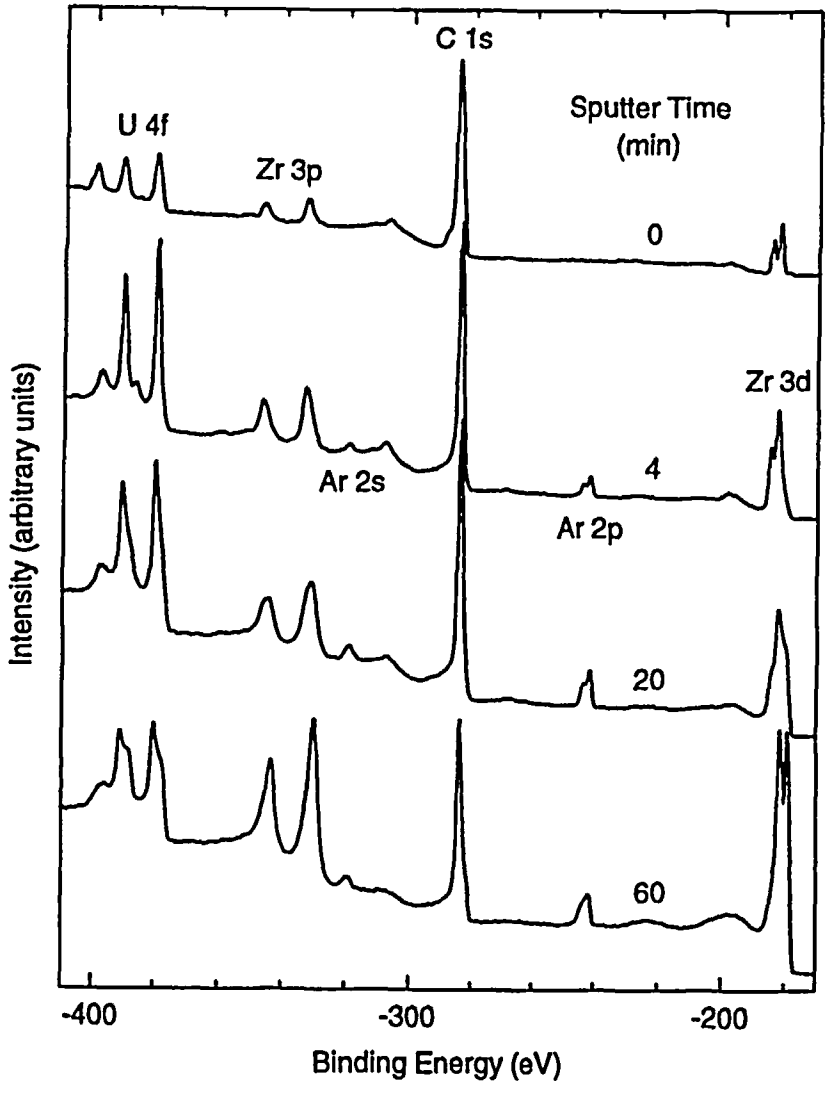

FIGURE 7. SERIES OF XPS SPECTRA RECORDED FROM A THIN-CANLUB LOCATION (SAME AS IN FIGURE 5) AFTER ARGON-ION SPUTTERING AS SPECIFIED.

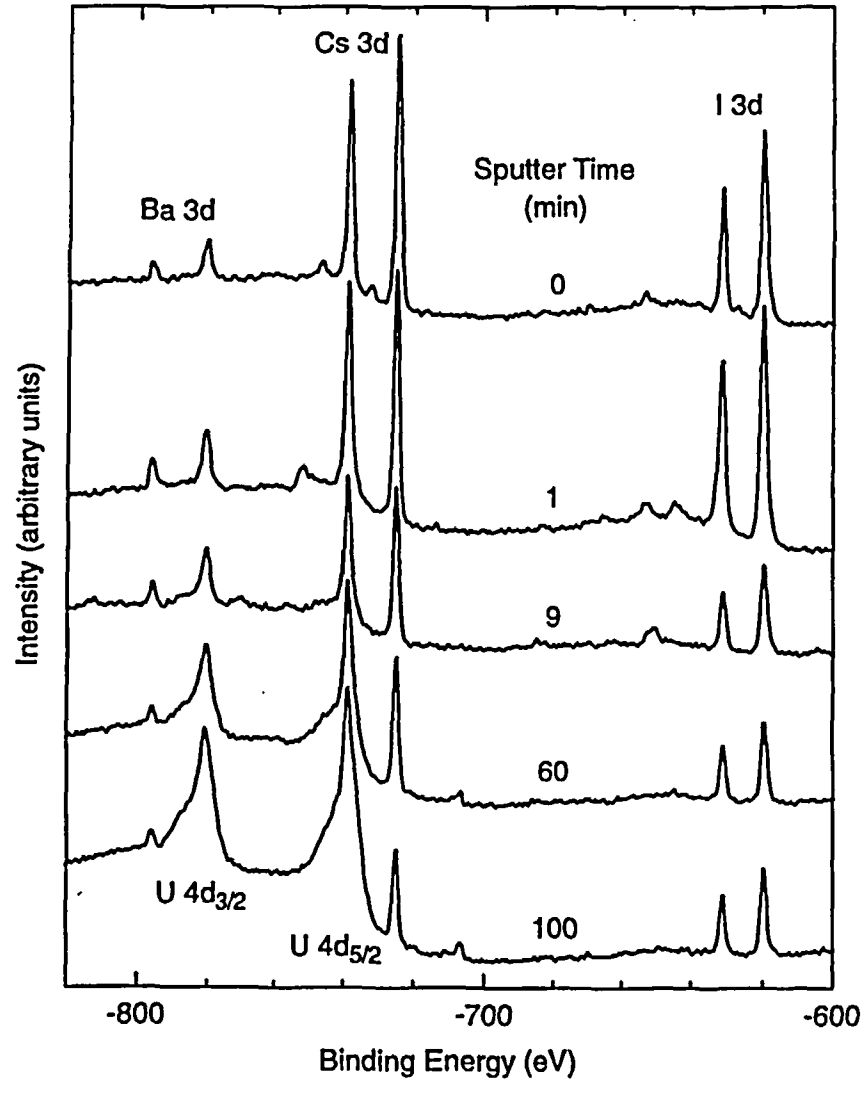

FIGURE 8. SERIES OF XPS SPECTRA RECORDED FROM THE SAME LOCATION AS FIGURE 6 AFTER ARGON-ION SPUTTERING AS SPECIFIED.

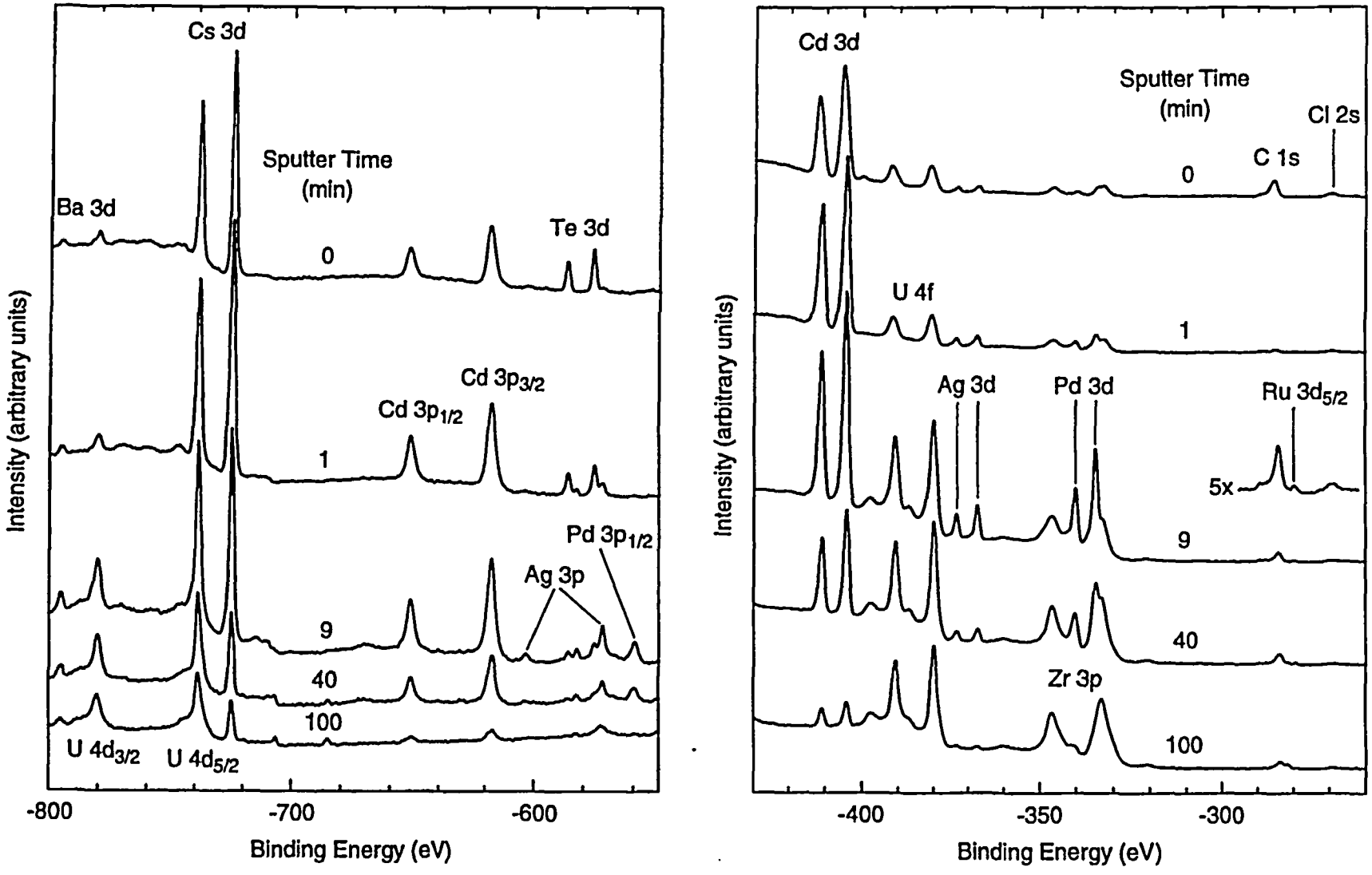

FIGURE 9. SERIES OF XPS SPECTRA RECORDED FROM A TYPICAL LOCATION ON THE END CAP AFTER ARGON-ION SPUTTERING AS SPECIFIED (HIGHER AND LOWER BINDING-ENERGY RANGES ON THE LEFT AND THE RIGHT RESPECTIVELY).